

Design Optimization of a Single-Phase Axial Flux Induction Motor with Low Torque Ripple

Abstract. Beside distinct advantages of single phase axial flux induction motors, they suffer from high torque ripple. In this paper a new detailed model of motor considering saturation, anisotropy and harmonics is developed. Then design optimization is done regarding low torque ripple using a new evolutionary algorithm which is called imperialist competitive algorithm. Not only geometrical dimensions, but also the temperature of different parts of motor is considered as constraints. Optimization results have been validated using three dimensional time-stepping finite element methods.

Streszczenie. W artykule analizowano tężnienia momentu napędowego w silniku indukcyjnym osiowym, jednofazowym. Wzieto pod uwagę indukcję nasycenia, anizotropię i obecność harmonicznych. Analizowano wymiary silnika oraz rozkład temperatury. (Optymalizacja osiowego silnika indukcyjnego pod kątem obecności tężnień momentu)

Keywords: Single-Phase Axial flux induction motor, Imperialist Competitive Algorithm (ICA), 3-D time stepping finite element analysis (FEA), thermal equivalent circuit.

Słowa kluczowe: silnik indukcyjny osiowy, tężnienia momentu napędowego.

Introduction

The special features of the axial flux machines such as their planar and adjustable air gap, better power to weight and diameter to length ratio, compact construction, and better efficiency, especially in a machine with a large number of poles (more than 12), make them an attractive alternative over conventional machines in a number of applications, such as fans, wheels, pumps, domestic applications and electrical vehicles [1-2]. Specially, in the field of small power domestic applications single-phase axial-field induction motors may have distinct advantages [3-4]. Firstly, the flat shape of AFM is a desirable configuration for the said applications. Secondly, the rotor may be integrated with the rotating part of mechanical load, e.g. the blades of fan, the impeller of pump, etc. The axial-force between stator and rotor is not so serious in small power range, thus it can be withstand by thrust bearing or by using ironless rotor disc and magnetic flux return path located at the opposite side of the rotor [3, 5].

Besides all above advantages, single phase axial flux induction motors such as conventional ones suffer from high torque ripples. This high torque ripple not only causes high noise generation in this motors, but also may increase the flux density harmonics and so power loss.

Design optimization of axial flux induction motors is considered in [3, 6-15]. In [3, 6] the optimization of diameter ratio with respect to the power and inertia has been presented. The approach of [7-10] is based on the general-purpose sizing equations. In these papers power density of the machine for a certain ratio of outer to inner diameter of machine is maximized. Authors of [11] have claimed that two optimization techniques were used in their paper: a geometrical optimization, and a structure analysis optimization. In the first optimization the weight of motor active material has been chosen as objective function. Then the weight variation versus frequency and diameter has been drawn. These figures give the minimum weight for the optimal frequency and diameter. In the second optimization, F.E.A. is used to analyze the flux distribution and to check the saturation of the machine structure in a nonlinear magneto-static model under no-load operating conditions. In [12-15] the effect of air-gap length, inverter switching frequency, and number of rotor slots on the performance of axial flux solid rotor induction motor have been presented.

It is to be noted that almost all of the previous works regard three phase axial flux induction motors with solid disk rotors and there is no paper on the design optimization

of laminated squirrel cage single phase induction motor. All optimizations have been carried out based on the variation of objective function with respect to the single variable and the effect of optimized value of variable on the other performance characteristics of motor have not been considered.

In this paper torque ripple of a single phase AFIM is minimized. It seems that by minimizing the total harmonic distortion (THD) of air-gap flux density (B_g) as an objective function, the torque pulsations can be minimized. So, minimization of THD is selected as an objective function. The ratio of outer to inner diameter, air gap length, stator, and rotor slot width and stator core depth are chosen as design variables of the first optimization problem. In the second problem, besides these geometrical dimensions, the temperature of stator, rotor, and air-gap are considered. Although axial-field machines possess a greater diameter-to-length ratio and their inner diameter will usually be much greater than the shaft diameter so they can be achieved better ventilation and cooling [3], in this paper the temperature of stator, rotor and air-gap of motor are considered in the optimization process. These values are calculated using a thermal equivalent circuit which is presented in this paper. Then, optimization is carried out by imperialist competitive algorithm (ICA) to find out the best set of design variables. Proposed method for optimization has some advantages, such as simplicity, accuracy, and time saving. After optimization its results are validate using 3-D time stepping finite element method (FEM).

Machine Modeling With Maxwell Equations

In machine modelling with Maxwell equations, the AFIM is divided to eight layers: air above stator, stator yoke, stator teeth and slots, air gap, equivalent rotor conducting layer, rotor teeth and slot, rotor yoke and air below rotor. Solving Laplace and Poisson equations in each layer gives flux density (B) and field intensity (H) in each point. A physical and layer model of AFIM is shown Fig. 1 and 2. In proposed model, each layer is characterized by its conductivity σ_i , relative permeability in the x and y directions to allow for anisotropy, μ_{xi} , μ_{yi} , and thickness d_i . The effect of stator and rotor teeth has considered using Carter's coefficient. Furthermore, the aluminium cage of rotor is supposed as an equivalent conducting layer and the winding of stator is considered using a thin current sheet. The density of this current will be [16]:

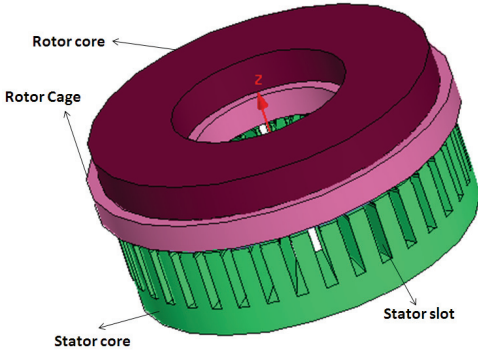


Fig. 1. Topology of a single phase AFIM (the stator winging is omitted for clarity)

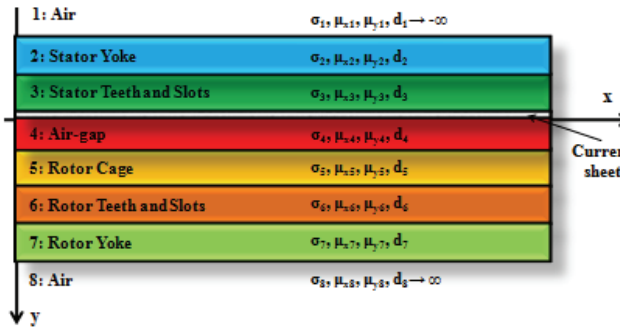


Fig. 2. A layer model of an axial flux induction motor

$$(1) J_s(x) = \sum_n -j \frac{2\pi n}{l} A_n \exp\left(j\left(\omega t - \frac{2\pi n}{l} x\right)\right)$$

Where $l=\pi (D_o+D_i)/4$, n is harmonic order and A_n is a value depend on the stator winding structure.

Maxwell equations in the different layers of the physical model are derived. The equations lead to Laplace and Poisson equations as follows:

$$(2) \frac{1}{\mu_{yi}} \frac{\partial^2 A_{zi,n}(x,y)}{\partial x^2} + \frac{1}{\mu_{xi}} \frac{\partial^2 A_{zi,n}(x,y)}{\partial y^2} = \sigma_i (j\omega A_{zi,n}(x,y) + U_{xi,n} \frac{\partial A_{zi,n}(x,y)}{\partial x})$$

The general solution of (2) is:

$$(3) A_{zi,n}(x,y) = [C_{i,n} \exp(\alpha_{i,n}y) + D_{i,n} \exp(-\alpha_{i,n}y)] \exp[j(\omega t - \beta x)]$$

Where

$$(4) \alpha_{i,n}^2 = \beta_n^2 \left(\frac{\mu_{xi}}{\mu_{yi}} + j \frac{\sigma_i \mu_{xi} (1-n(I-s)U_s)}{n \beta_n} \right)$$

Furthermore, the components of the magnetic flux density can be obtained from the definition, $\nabla \times \vec{A} = \vec{B}$

$$(5) B_{xi,n} = \frac{\partial A_{zi,n}}{\partial y} = \alpha_{i,n} [C_{i,n} \exp(\alpha_{i,n}y) + D_{i,n} \exp(-\alpha_{i,n}y)] \exp[j(\omega t - \beta x)]$$

$$(6) B_{yi,n} = -\frac{\partial A_{zi,n}}{\partial x} = j\beta_n [C_{i,n} \exp(\alpha_{i,n}y) + D_{i,n} \exp(-\alpha_{i,n}y)] \exp[j(\omega t - \beta x)]$$

The coefficients of $C_{i,n}$ and $D_{i,n}$ can be calculated considering the following boundary conditions [17]:

- 1) B_y is continuous
- 2) All field components disappear at $y = \pm\infty$
- 3) If a current sheet, J_s , lies between two layers (i) and ($i+1$) then $H_{x(i+1)} - H_{xi} = J_s$

Finally, the flux density in middle of the magnetic air gap has only a normal component given by:

$$B_{y4,n}(x) =$$

$$(7) \sum_{n=1,3,\dots}^{\infty} j\beta_n \left(\left(C_{4,n} e^{\frac{\alpha_{4,n}g}{2}} + C_{2,n} e^{-\frac{\alpha_{4,n}g}{2}} \right) e^{j(\omega t - \beta_n x)} \right)$$

The fundamental component of the air-gap flux density, as well as its harmonics, can be obtained using Eq. (7).

The torque of the motor will be calculated as [16]:

$$(8) T = r_{mean} \cdot h \cdot \text{Real} \left\{ \int_0^l \frac{B_{y4,n} B_{x4,n}^*}{2\mu_0} dx \right\}_{y=d_s}$$

And the inductive current in the rotor is:

$$(9) J_{r,n} = \sigma_i \left(-\frac{\partial A_{zi,n}}{\partial t} - U_{xi} \frac{\partial A_{zi,n}}{\partial x} \right)$$

Further details of proposed model will be published in next paper.

Optimization Problem

A. Objective Function and Constraints

The studied motor is a single phase capacitor-run axial flux induction motor. The geometric parameters of the original motor are presented in Table 1.

Table 1. The parameters of studied AFIM

Parameter	Unit	Value
Output power	Hp	3/4
Frequency	Hz	50
Voltage	V	220
Capacitor	μF	6.3
Pole pair	-	3
Slip	%	4
Air gap length	mm	2
Core outer /inner diameters	mm	170/87
Core length, stator/rotor	mm	15/19
Number of slots, stator/rotor	-	36/45
Stator slot:	mm	6.5
B_{s1}		5.5
B_{s2}		1
H_{s0}		2
H_{s1}		28
Rotor slot:	mm	1
B_{s0}		3
B_{s1}		5
B_{s2}		0.5
R_s		1
H_{s0}		1
H_{s1}		11
Skew, stator/rotor	degree	0/8

It seems that by minimizing the total harmonic distortion (THD) of B_g as an objective function, the torque pulsations can be minimized. So, total harmonic distortion (THD) of B_g is defined as:

$$(10) THD = \text{sqrt} \left(\sum_{n=3,5,\dots}^{\infty} B_{y4,n}^2 \right) / B_{y4,1}$$

The design variables of optimization problem are chosen as air gap length, the ratio of outer to inner diameter of core, stator, and rotor slot width, and depth of stator core.

A number of constraints can also be taken into account during the optimization to prevent the possibility of reaching unrealistic optimization results. For example, the air gap is limited since a large air gap leads to a reduction in the motor torque. A small air gap, on the other hand, causes mechanical faults and manufacturing difficulties. Stator and rotor slot width is limited with the maximum and minimum tooth width which is determined with allowed tooth flux density. Finally, lower bound of torque is chosen close to its initial values of the non-optimized motor. Therefore, we can be sure that neither the torque average nor its pulsations has been deteriorated.

The optimization is carried out in two cases. In optimal design 1, just geometrical dimensions are used as design constrains while in optimal design 2 beside them, stator, rotor, and air-gap temperature rise are regarded. The maximum value of this new constrains are chosen close to their initial values which are calculated using simple equivalent circuit of fig. 3.

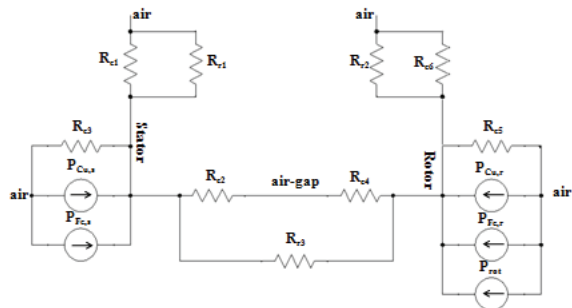


Fig. 3. Thermal equivalent circuit of AFIM

In this figure, R_{c2} is the convection heat transfer resistance between the stator and air flow in the air gap which is calculated as [18]:

$$(11) \quad R_{c2} = R_{c4} = 4 / (h_{rs} \times \pi (D_o^2 - D_i^2))$$

Where h_{rs} is the average heat transfer coefficient between two discs. The radiation heat transfer resistance between the stator and rotor discs is [18]:

$$(12) \quad R_{r3} = \left(\frac{1 - \varepsilon_1}{\varepsilon_1 A_1} + \frac{1}{F_{12} A_1} + \frac{1 - \varepsilon_2}{\varepsilon_2 A_2} \right) / (\sigma [(\theta_1 + 273) + (\theta_2 + 273)] \times [(\theta_1 + 273)^2 + (\theta_2 + 273)^2])$$

In which the areas of both discs can be taken as the same,

$$(13) \quad A_1 = A_2 = \pi (D_o^2 - D_i^2) / 4$$

And $F_{12}=1$ is the shape factor; ε_1 and ε_2 are the emissivity of stator and rotor respectively. In this analysis the radiation heat transfer resistance between both stator and rotor with air is ignored.

The convection heat transfer resistance at the outside surface of the disc is [18]:

$$(14) \quad R_{c3} = R_{c5} = 4 / (h_{fr} \pi D_o^2)$$

Where h_{fr} is the average heat transfer coefficient at the outer surface of the disc and finally the convection heat transfer resistance at the periphery of the stator/rotor is [18]:

$$(15) \quad R_{c1} = R_{c6} = (h_p \pi D_o d)^{-1}$$

Where h_p is average heat transfer coefficient around the radial periphery.

B. Optimization Method

Imperialist Competitive Algorithm (ICA) is a new evolutionary algorithm for optimization. This algorithm starts with an initial population. Each population in ICA is called country. Countries are divided in two groups: imperialists and colonies. In this algorithm the more powerful imperialist, have the more colonies. When the competition starts, imperialists attempt to achieve more colonies and the colonies start to move toward their imperialists. So during the competition the powerful imperialists will be improved and the weak ones will be collapsed. At the end just one imperialist will remain. In this stage the position of imperialist and its colonies will be the same. The flowchart of this algorithm is shown in fig. 4 [19]. More details about this algorithm are presented in [19].

Table 2. Design Constrains

Parameter	Unit	Minimum Value	Maximum Value
air gap length	mm	0.9	3
stator slot width	mm	5	10
rotor slot width	mm	3	8
depth of stator core	mm	10	20
the ratio of outer to inner diameter of core	-	1.1	3
Motor torque	N.m.	6.2	-
Stator temperature rise	°C	-	42
rotor temperature rise	°C	-	37
Air-gap temperature rise	°C	-	29

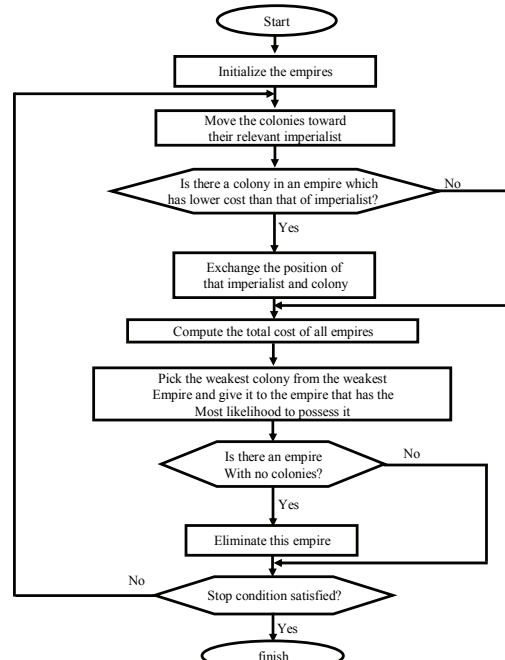


Fig. 4. Flowchart of the Imperialist Competitive Algorithm (ICA) [19].

As mentioned before in this optimization problem the objective function is the inverse of (23). Optimization variables are the ratio of outer to inner diameter, air gap length, stator, and rotor slot width and stator core depth. The number of countries is 200 and the number of imperialists is 8.

Results

ICA is used to optimize the design of a typical single phase axial flux induction motor. Optimization is done in two cases, resulting different designs.

Design variables in these cases are listed in table 3. Table 4 and fig. 5 show the characteristics of motor in the different optimization problems and those of typical motor.

It can be seen in table 4 and fig. 5 that the typical motor has the THD of 21.66% while its average developed torque is 6.3 N.m. Optimal design 1 is carried out considering THD of By as objective function. In this optimization THD is reduced to 4.57% while developed torque is the same as typical motor. Because the temperature rise of motor is not considered in the optimization process, it is deteriorated. The maximum temperature rise (in the stator) in optimal design1 is about 11.95% more than typical one.

In optimal design 2 the temperature rise of motor is considered as additional constrains in the optimization process. The results of this optimization show although THD is improved about 56.57% against typical motor, it is collapsed with respect to optimal design 1. On the other hand, maximum temperature rise of motor is decreased with respect to optimal design 1 and it is close to that of typical motor. This proves the effectiveness of the proposed optimization in simultaneously meeting the entire objective and constrains.

Table 3. Dimensions of optimized motor for different objective functions

Parameter	unit	Typical motor	Optimal Design 1	Optimal Design 2
air gap length	mm	2	3	3
stator slot width	mm	5.5	10	7
rotor slot width	mm	5	8	6
depth of stator core	mm	15	15	20
outer / inner diameter of core	-	1.954	1.45	1.84

Table 4. The characteristics of optimized motor

Parameter	unit	Typical motor	Optimal Design 1	Optimal Design 2
THD	%	21.66	4.57	13.66
Developed Torque	N.m.	6.3	6.3	6.2
Stator Temp. rise	°C	40.5	45.34	41.24
Rotor Temp. rise	°C	36.08	39.48	36.59
Air-gap Temp. rise	°C	28.53	28.72	28.59

3-D time stepping finite element analysis

The finite element solution of magnetic field problem was originally proposed by Sylvester and Chari and nowadays, it is regarded as one of the most powerful tools in electromagnetic analysis [20].

On the other hand, it is mentioned in [21] that the disk-like structure of the stator and rotor cause the magnetic field to be non-uniformly distributed within the volume of the motor, particularly in the motor stator core. This is the main reason why the magnetic field should be calculated in three dimensional (3-D) spaces. Furthermore, in order to describe the performance of induction motor with a good accuracy, it is essential to consider both saturation and eddy current effects simultaneously. So, in this section 3-D time stepping finite element method (FEM) is employed to validate the optimization results.

The graphical representation of calculated mesh in the analyzed AFIM is shown in fig. 6. Figs. 7 and 8 regard the

peripheral and radial components of flux density magnitude in the air-gap of typical and optimal motor 2.

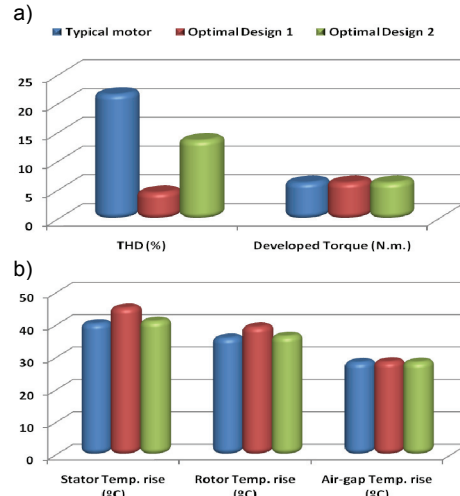


Fig. 5. The characteristics of the typical and optimized motors

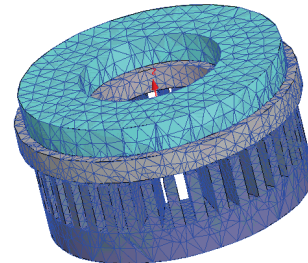


Fig. 6. graphical representation of calculated mesh in the analyzed AFIM

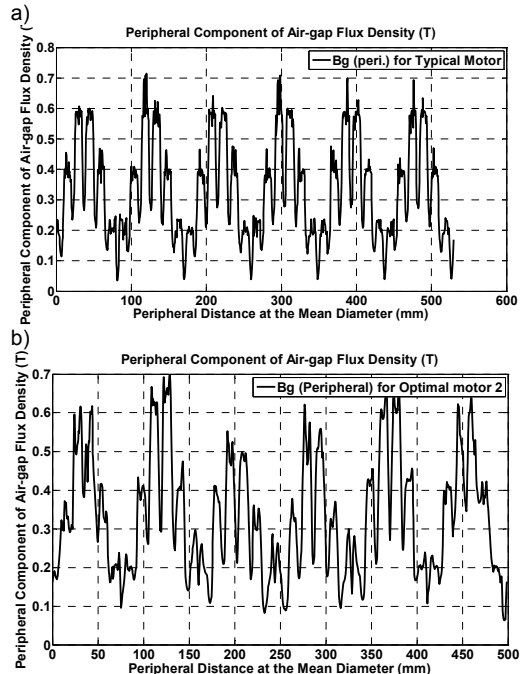


Fig.7. the peripheral component of flux density magnitude in the outer diameter of air-gap for (a) typical and (b) optimal motors

Conclusions

Axial flux induction motors have many advantages that cause to increase their application. But they have a major disadvantage in the single phase operation, high torque

pulsation. In this paper imperialist competitive algorithm is used to optimize total harmonic distortion of air gap flux density to minimize torque pulsation. Optimization is done in two cases. At first just the geometrical dimensions of motor are considered in the optimization which leads to a sharp decrease in THD and simultaneously an increase in temperature rise of motor. In the second design stator, rotor and air-gap temperatures are superimposed to the first constraints and the optimization is repeated. Although THD of By in optimal design 2 is more than that of optimal design 1, it is less than that of typical motor and furthermore the temperature rise of motor is close to that of typical motor. In both optimizations developed torque of motor is chosen as constrain to be sure it is not deteriorated in the optimizations. Finally 3-D time stepping finite element analysis is used to validate optimization process.

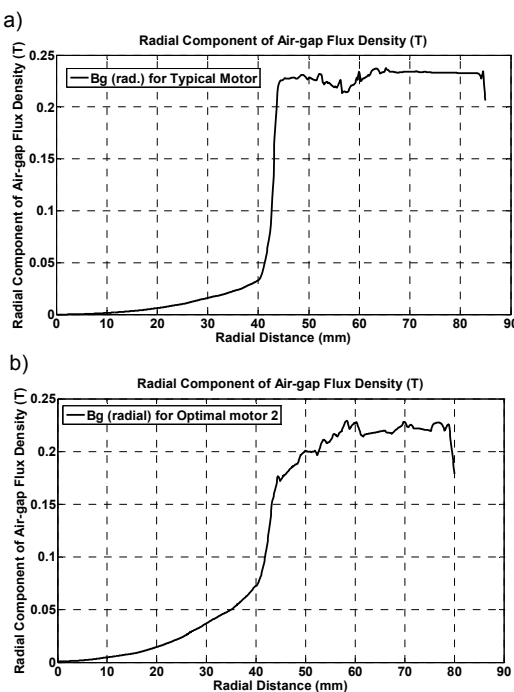


Fig. 8. the radial component of flux density magnitude in the air-gap of (a) typical and (b) optimal motors

REFERENCES

- [1] Valtonen M., Parviainen A. and Pyrhonen J., "Electromagnetic Field Analysis of 3D Structure of Axial-Flux Solid-Rotor Induction Motor", SPEEDAM 2006, International Symposium on Power Electronics, Electrical Drives, Automation and Motion, S39-12 –S39-16, 2006.
- [2] Wallace R., Mopan L., Cea G., Perez F., "Design and Construction of Medium Power Axial Flux Induction Motors", 260-265.
- [3] Leung W. S., Chan J.C.C., "Axial-Field Electrical Machines-Design and Application", *IEEE Trans. on Power Apparatus and Systems*, PAS-99(1980), No. 4, 1679-1685.
- [4] Chan C.C., "Single-phase axial-field motor for ceiling fan drives", Proceedings CNR International Symposium on Electrical Machines for special purposes, 1981, 63-71.
- [5] Clark R.J., "Development in- alternating current induction motors", British Patent No. 1465268.
- [6] Leung W.S., Chan C.C., "A New Design Approach For Axial-Field Electrical Machines", *IEEE Transactions on Power Apparatus and Systems*, PAS-99(1980), No. 4, 1679-1685, July/Aug 1980.
- [7] Huang S., Luo J., Leonardi F. and Lipo T. A., "A General Approach to Sizing and Power Density Equations for Comparison of Electrical Machines", IEEE Conference 1996, 836-842.
- [8] Surong H., Guodong X., "Optimization of Power Density for Axial-Flux Machine through Generalized Sizing Equations" *Journal of Shangiiai University*, 1(1997), No. 3, 232-236, Dec. 1997.
- [9] Huang S., Luo J., Leonardi F. and Lipo T. A., "A General Approach to Sizing and Power Density Equations for Comparison of Electrical Machines", *IEEE Transaction on Industry Applications*, 34(1998), No. 1, 92-97, Jan./Feb. 1998.
- [10] Huang S., Luo J., Leonardi F., Lipo T. A., "A Comparison of Power Density for Axial Flux Machines Based on General Purpose Sizing Equations", *IEEE Transactions on Energy Conversion*, 14(1999), No. 2, 185-192, June 1999.
- [11] Benoudjitt A., Guettaf A., Nait Saïd N., "Axial Flux Induction Motor for On-Wheel Drive Propulsion System", *Electric Machines and Power Systems*, 28(2000), Taylor & Francis, 1107-1125, 2000.
- [12] Valtonen M., "Performance Characteristics of an Axial-Flux Solid-Rotor-Core Induction Motor", Phd thesis, Lappeenranta University of Technology, Lappeenranta, Finland, 2007.
- [13] Valtonen M., Parviainen A. and Pyrhonen J., "Influence of the Air-Gap Length to the Performance of an Axial-Flux Induction Motor", Proceedings of the 2008 International Conference on Electrical Machines, 1-5, 2008.
- [14] Valtonen M., Parviainen A. and Pyrhonen J., "Inverter Switching Frequency Effects on the Rotor Losses of an Axial-Flux Solid-Rotor Core Induction Motor", Powereng 2007, April 12-14, 2007, Setubal, Portugal, pp. 476-480.
- [15] Valtonen M., Parviainen A. and Pyrhonen J., "The Effects of the Number of Rotor Slots on the Performance Characteristics of Axial-Flux Aluminium-Cage Solid-Rotor Core Induction", IEEE Conference, pp. 668-672, 2007.
- [16] Mirzayee M., Mirsalim M., and Abdollahi S.B., "Presentation of analytical and finite element methods for analysis of a disk induction motor performance", *the journal of Amir-Kabir university*, 15(2004), No. 58-A, 244-257, (in Persian).
- [17] Idir K., Dawson G. E., and Eastham A. R., "Modeling And Performance of Linear Induction Motor with Saturable Primary", *IEEE Trans. on Industry Applications*, 29 (1993), No. 6, 1123-1128.
- [18] Gieras J. F., Wang R., Kamper M. J., "Axial Flux Permanent Magnet Brushless Machines", Springer Science, Second Edition, 2008.
- [19] Atashpaz-Gargari E., Lucas C., "Imperialist Competitive Algorithm: An Algorithm for Optimization Inspired by Imperialistic Competition", IEEE conference CEC, 2007.
- [20] Chan C.C., "Design of electrical machines by the finite element method using distributed computing", Elsevier, *Computers in Industry*, 17 (1991), 367-374.
- [21] Lukaniszyn M., Jagiela M., Wrobel R., "A disc type motor with co-axial flux in the stator influence of magnetic circuit parameters on the torque", Springer-Verlag, Electrical Engineering 84 (2002), 91-100.

Authors: Zahra Nasiri-Gheidari, Ph.D. Student, School of Electrical and Computer Engineering, Faculty of Engineering, University of Tehran, North Kargar Ave., P.O. Box: 14395/515, Tehran, Iran, E-mail: z_Nasiri@ee.sharif.edu; Prof. dr. Hamid Lesani, Center of Excellence on Control and Intelligent Processing, School of Electrical and Computer Engineering, Faculty of Engineering, University of Tehran, North Kargar Ave., P.O. Box: 14395/515, Tehran, Iran, E-mail: Lesan@ut.ac.ir